



**ISTITUTO NAZIONALE DI FISICA NUCLEARE**

**Sezione di Genova**

---

**INFN/AE-00/04**

**17 Febbraio 2000**

## **DETAILED FIELD DISTRIBUTION IN CMS WINDING**

S. Farinon, P. Fabbriatore, R. Musenich

*INFN-Sezione di Genova, Via Dodecaneso 33, I-16146 Genova, Italy*

### **Abstract**

The CMS winding has now arrived at its constructive phase. This means that some practical aspects regarding the winding itself have to be considered, such as the minimum requirement of conductor performance for each layer of each module. Several magnetic calculations have been already performed, but the winding has been never analyzed in detail, in order to understand the impact of the self-field on its performances.

This analysis and its implications are reported in this paper.

*Published by SIS-Pubblicazioni  
Laboratori Nazionali di Frascati*

## 1 INTRODUCTION

The CMS winding has now arrived at its constructive phase. This means that some practical aspects regarding the winding itself have to be fixed: for instance, the minimum critical current of the strands have to be decided, and the modules needing the best quality cables have to be determined.

In this frame, a 2D magnetic analysis has been performed using the finite element (FE) code ANSYS®.<sup>1)</sup> The high grade of accuracy of the model allows to compute the field in each turn of the winding: as it will be shown in the next sections, this information is very significant for the winding final quality and behavior.

## 2 MAGNETIC FINITE ELEMENT MODEL

The CMS winding is made by 5 modules, named CB-2, CB-1, CB0, CB+1 and CB+2 moving from backward to forward. Each module is then constituted by 4 layers, numbered from the internal to the external one, and each layer is then made by 110 turns. The CMS magnet has been modeled as shown in Fig. 1; due to its symmetry only half the model, axially, has been simulated. All the Rutherford cables, 110 per module per layer, have been meshed by a 2D axisymmetric element. The iron has been modeled with its non-linear magnetic property.

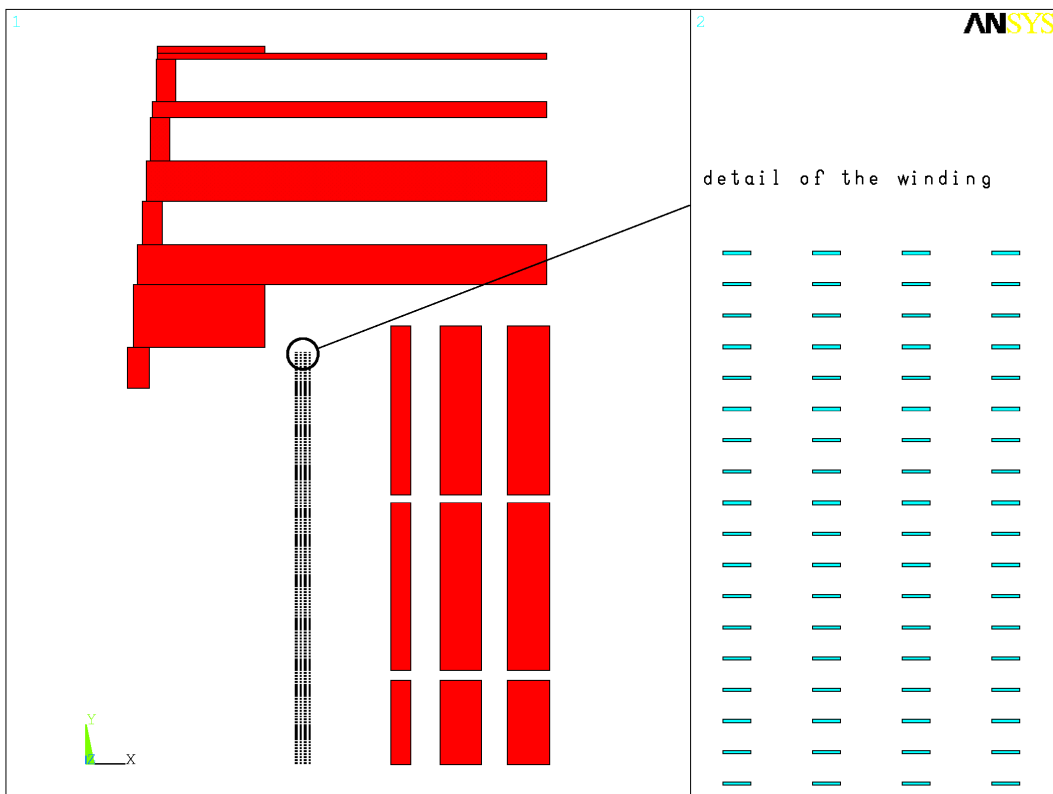


**FIG. 1:** 2D model of the CMS magnet, with meshing of every conductor.

### 3 FIELD IN THE WINDING

The result in terms of magnetic field is shown in Fig. 2. The central magnetic field, as expected, is 4.06 T, corresponding to an operating current of 19500 A.

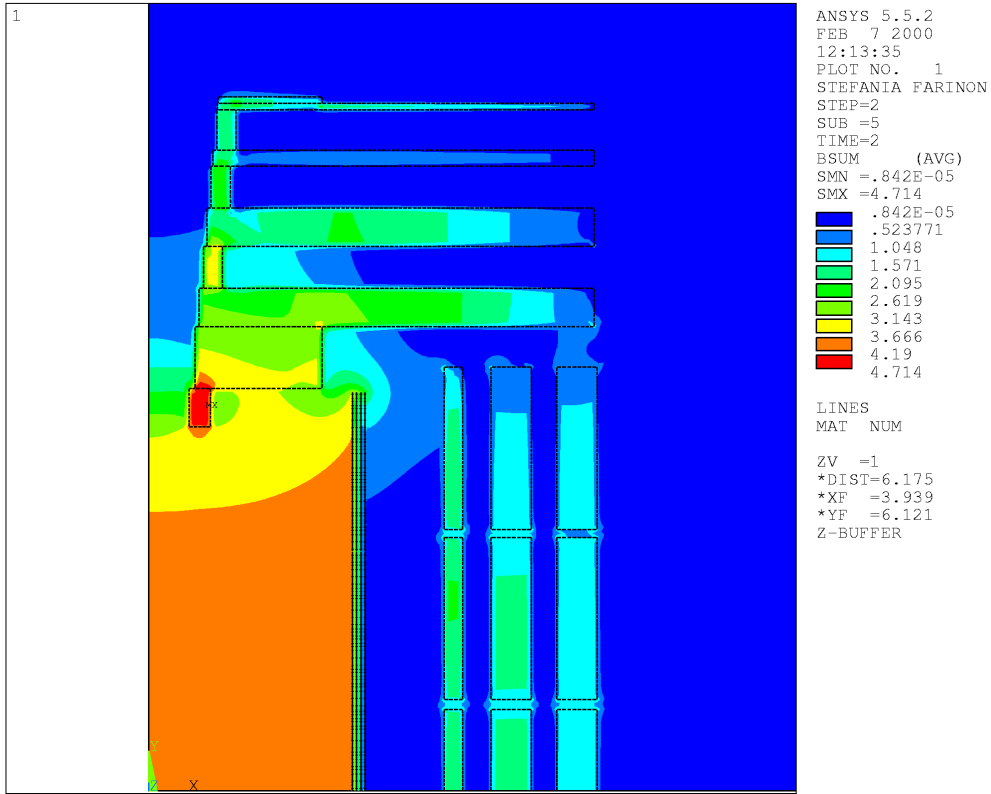


**FIG. 2:** General map of magnetic field.

In order to understand the detailed magnetic field results, a schematic view of the mesh of the Rutherford cables is shown in Fig. 3. Each Rutherford cable has been meshed with one axisymmetric element made by 8 nodes, 4 corner nodes + 4 midside nodes. The midside nodes allow a more accurate calculation, but no result is available at their locations.

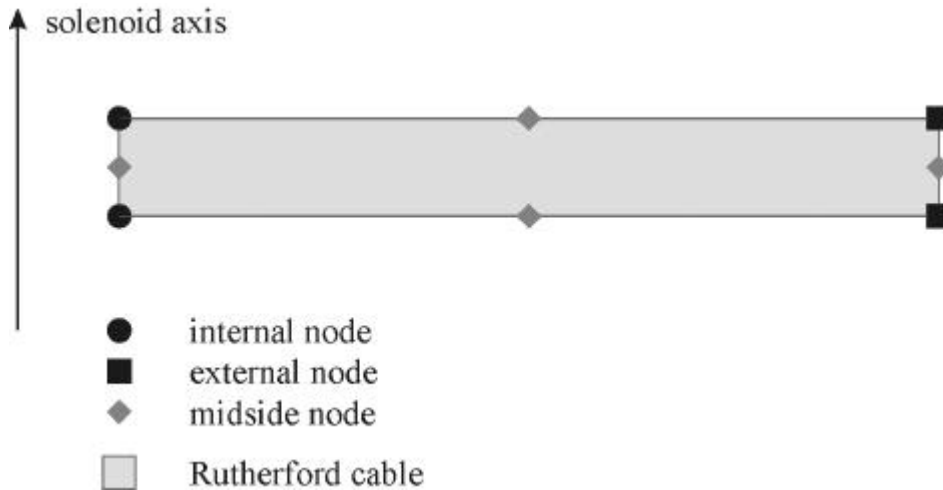


**FIG. 3:** Scheme of the mesh of the Rutherford cables.

Therefore, the magnetic field is mapped at the four corner nodes of each Rutherford cable. The corner nodes can be subdivided into two groups: the internal nodes, made by the 2 corner nodes of each cable of each layer at the inner radius, and the external ones, made by the 2 corner nodes of each cable of each layer at the outer radius.

Finally, three meaningful plots are possible, as function of the distance from the midplane of the magnet:

- average magnetic field on each element (one value each Rutherford cable);
- magnetic field on the internal nodes;
- magnetic field on the external nodes.

In Fig. 4 the magnetic field averaged on each element is shown. For the central (CB0) and first module (CB+1 and symmetrically CB-1) the magnetic field is nearly constant on each layer and corresponds to about 3.5 T, 2.5 T, 1.5 T and 0.5 T, respectively for the 1<sup>st</sup>, 2<sup>nd</sup>, 3<sup>rd</sup> and 4<sup>th</sup> layer. The last turns of the external modules (CB+2 and CB-2) are more critical, since the field dramatically increase up to 3 T in every layer.

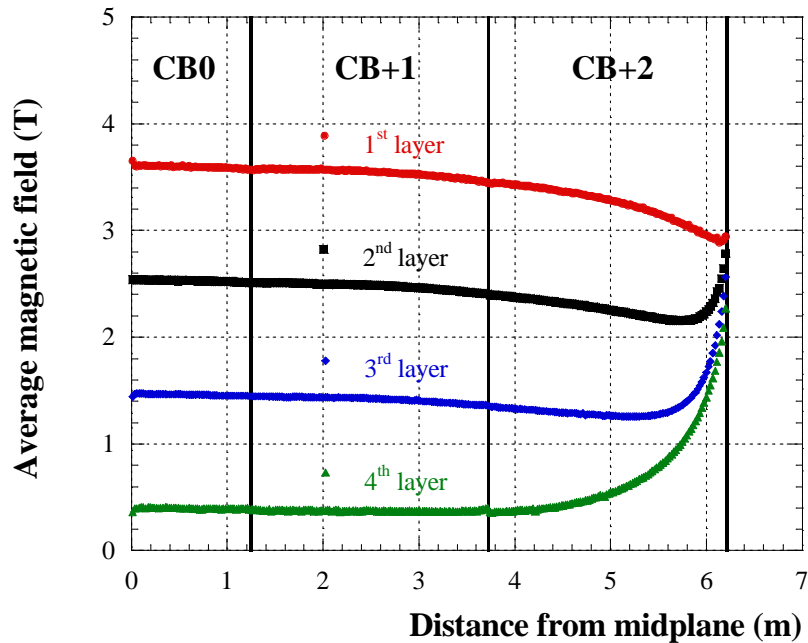


**FIG. 4:** Average magnetic field on each Rutherford cable as function of the distance from the magnet midplane.

More detailed information is given by Figs. 5 and 6, showing respectively the magnetic field on the internal nodes and on the external ones as function of the distance from the magnet midplane. As it is clear from the figures themselves, the magnetic field behaves nearly in the same way in the inner and outer side of each Rutherford cable, the main difference being that it is higher on the nodes at inner radius. Therefore, let us concentrate on Fig. 5. In the central and first modules, the field is nearly constant on every layer, and assumes the values of about 4.3 T, 3.2 T, 2.15 T and 1.1 T, respectively for the 1<sup>st</sup>, 2<sup>nd</sup>, 3<sup>rd</sup> and 4<sup>th</sup> layer.

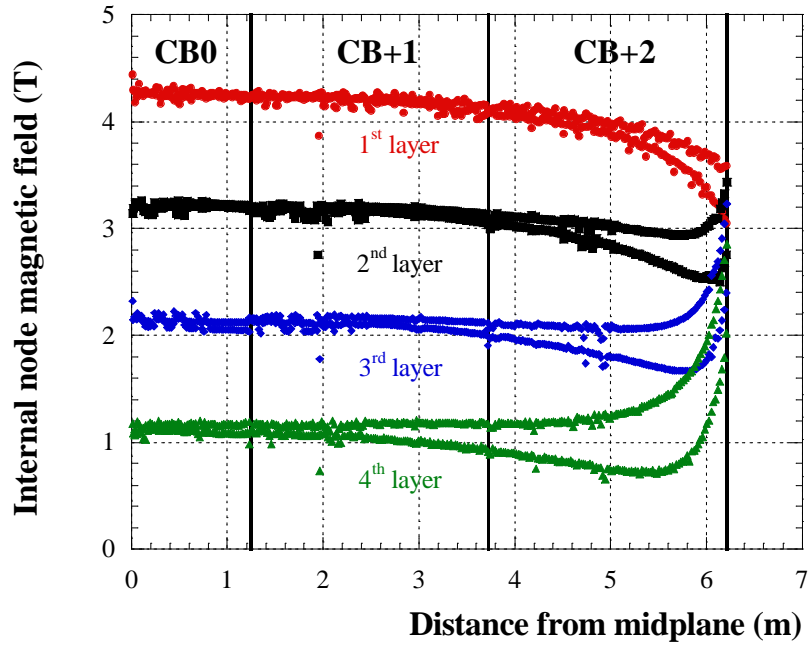


FIG. 5: Magnetic field on the internal nodes of each Rutherford cable of each layer as function of the distance from the magnet midplane.

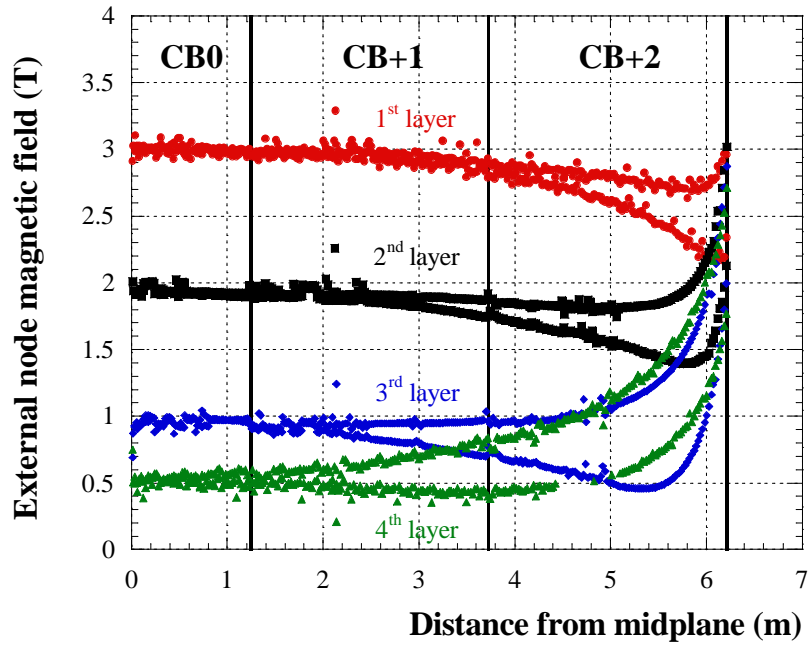
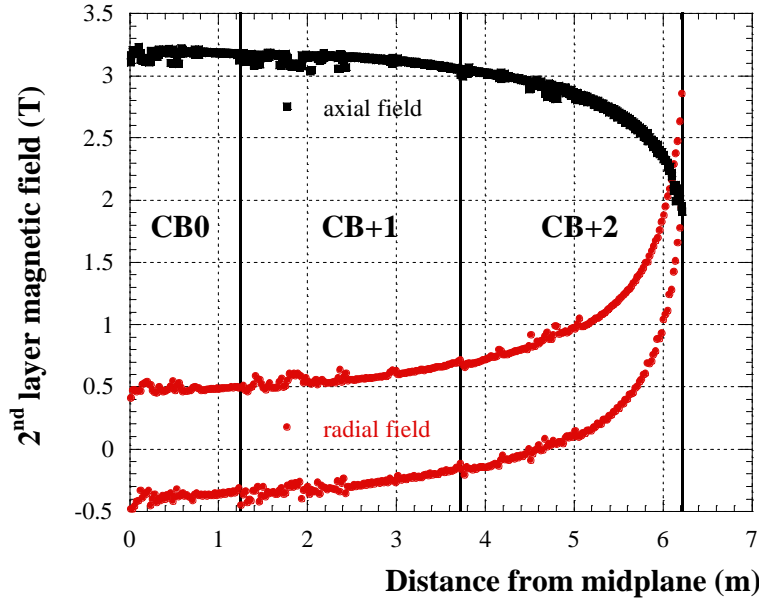


FIG. 6: Magnetic field on the external nodes of each Rutherford cable of each layer as function of the distance from the magnet midplane.

The magnetic field on each layer of the external modules (CB+2 and CB-2) behaves quite differently. There is a split in all the curves of the external modules independently from the layer. This is clearly due to the radial component of the magnetic field. Let us consider for instance the internal nodes of the 2<sup>nd</sup> layer. Fig. 7 shows the radial and axial component of the magnetic field of the 2<sup>nd</sup> layer as function of the distance from the magnet midplane. The axial component is fairly constant on the central and first modules, and significantly decreases on the external modules. The radial component has a different behavior: it is strongly higher on the lower side of each Rutherford cable than on the upper one. The result is that on the central and first modules, since the radial component is negligible, the axial component dominates and the magnetic field is nearly constant, whilst on the external modules the radial component is of the same order or even higher than the axial one, inducing the split on the total magnetic field as well.



**FIG. 7:** Radial and axial component of the magnetic field on the internal node of the 2<sup>nd</sup> layer as function of the distance from the magnet midplane.

The main result of this analysis, shown in Tab. 1, is to determine the maximum values assumed by the magnetic field and their location in the winding.

**TAB. 1:** Peak field in the winding.

|             | 1 <sup>st</sup> layer | 2 <sup>nd</sup> layer | 3 <sup>rd</sup> layer | 4 <sup>th</sup> layer |
|-------------|-----------------------|-----------------------|-----------------------|-----------------------|
| Module CB0  | 4.4                   | 3.3                   | 2.3                   | 1.2                   |
| Module CB+1 | 4.3                   | 3.2                   | 2.2                   | 1.2                   |
| Module CB+2 | 4.2                   | 3.4                   | 3.2                   | 2.9                   |

In fact, each layer of each module will be wound by a unique length, 2.5 Km long, of conductor. The goal is to use the best quality lengths, in terms of critical current degradation, in the layers at higher magnetic field. In Tab. 2 a sort of classification of the lengths, from the better to the worse, to be used in the winding is shown. This classification should be followed as carefully as possible, considering that all the lengths will not be available contemporary, but will be produced parallel to the winding operations, and the first module to be wound is the CB-2, one of the most critical.

**TAB. 2:** Order of best quality lengths to be used in the winding.

|    | layer           | module          |
|----|-----------------|-----------------|
| 1  | 1 <sup>st</sup> | CB0             |
| 2  | 1 <sup>st</sup> | CB+1 (and CB-1) |
| 3  | 1 <sup>st</sup> | CB+2 (and CB-2) |
| 4  | 2 <sup>nd</sup> | CB+2 (and CB-2) |
| 5  | 2 <sup>nd</sup> | CB0             |
| 6  | 2 <sup>nd</sup> | CB+1 (and CB-1) |
|    | 3 <sup>rd</sup> | CB+2 (and CB-2) |
| 7  | 4 <sup>th</sup> | CB+2 (and CB-2) |
| 8  | 3 <sup>rd</sup> | CB0             |
| 9  | 3 <sup>rd</sup> | CB+1 (and CB-1) |
| 10 | 4 <sup>th</sup> | CB0             |
|    | 4 <sup>th</sup> | CB+1 (and CB-1) |

Since the CMS solenoid will be wound internally, starting from the 4<sup>th</sup> layer to the 1<sup>st</sup> one, there is some margin to put the best quality lengths in the 1<sup>st</sup> layer of each module. Anyway, the lengths should be classified very carefully, to obtain the better distribution of lengths inside the winding.

## 4 IMPACT ON STABILITY

Being known the magnetic field on each cable, some useful information on the stability of the winding can be easily deduced. The stability of the winding is defined as the ability of the coil to support local or distributed temperature rises over the nominal temperature without quenching.

### 4.1 Critical temperatures

The critical temperature with no current flowing in the conductor,  $T_c$ , only depends on the magnetic field. For NbTi the critical temperature depends on field according to:

$$T_C(B) = T_{C0} \left( 1 - \frac{B}{B_{C20}} \right)^{0.59}, \quad (1)$$

where  $T_{C0}=9.3$  K is the critical temperature at  $B=0$ , and  $B_{C20}=13.9$  T is the critical field at  $T=0$ . Considering now that a current  $I_0$  flows in the conductor, a new critical temperature  $T_g$  is defined, as the maximum temperature for which the current  $I_0$  can flow with no dissipation in the superconducting part.  $T_g$  is called *current sharing temperature* and is defined by

$$T_g = T_C - (T_C - T_0) \frac{I_0}{I_C(T_0, B)}, \quad (2)$$

where  $I_C(T_0, B)$  is the critical current at nominal temperature ( $T_0=4.5$  K) and peak field. For CMS the operating current  $I_0$  is 19500 A, while the nominal critical current  $I_C$ , for instance at  $B=4.6$  T, is 55700 A.

## 4.2 Temperature margin

Now it is possible to define the temperature margin  $\Delta T$ , as the difference between the sharing temperature  $T_g$  and the nominal temperature  $T_0$ . It represents the maximum temperature raise every single turn could experience without quenching.

Fig. 8 represents the temperature margin calculated at the peak field of each Rutherford cable as function of the distance from the magnet midplane. In the CMS Engineering Design Review<sup>2)</sup> it was stated that this margin should be at least 1.85 K. The result of the finite element calculation shows that the most of the turns stay well over 1.85 K, the most critical region being again the first layer of each module ( $\Delta T=1.87$  K is the lower value).

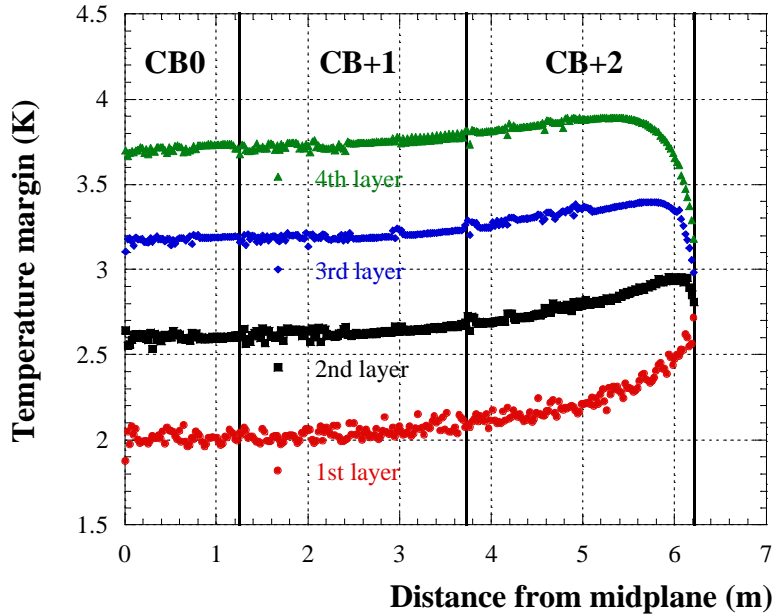


**FIG. 8:** Temperature margin  $\Delta T=T_g-T_0$  calculated at the peak field of each Rutherford cable as function of the distance from the magnet midplane.



It should be stressed that in Fig. 8 the temperature margins have been computed considering the nominal critical current curve. In case of particularly degraded cables, those margins could be considerably lower. Here again there is the need to put the conductors with the higher critical current in the most critical region, i.e. the ones with the lower values of temperature margins.

## 5 CRITICAL CURRENT

From the point of view of the critical current, it could be interesting to calculate the minimum critical current each Rutherford cable should support, considering the safe temperature margin  $\Delta T=1.85$  K reported in the EDR. The results are shown in Fig. 9. All the required minimum critical current values are lower than the nominal value of 55.7 kA at 4.6 T, also considering that the peak magnetic field is 4.4 T. The main implication is that, in the 2<sup>nd</sup>, 3<sup>rd</sup> and 4<sup>th</sup> layer, it is possible to tolerate critical current even 10% lower than its nominal value.

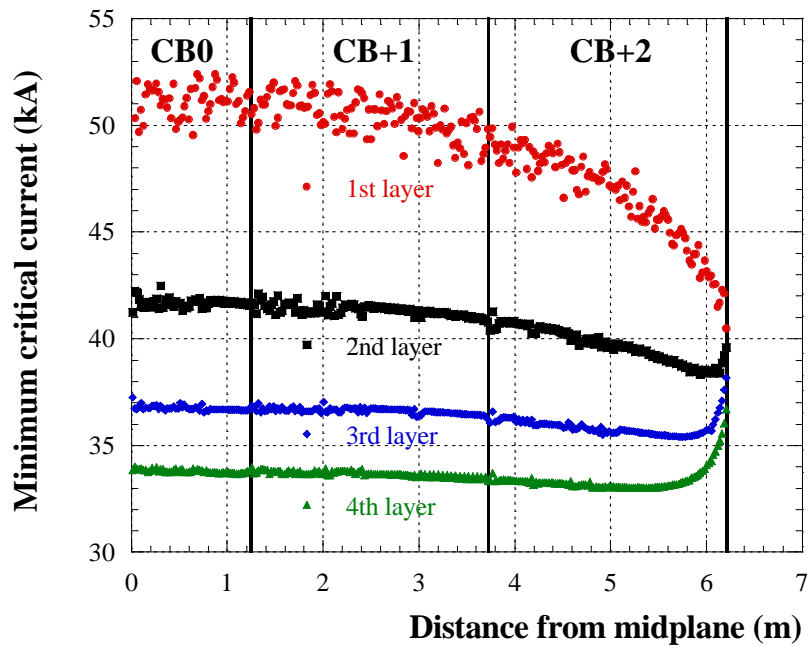


**FIG. 9:** Minimum critical current as function of the distance from the magnet midplane and corresponding to the minimum temperature margin  $\Delta T=1.85$  K, as stated in the EDR.

Imposing the condition that no conductor had a critical current lower than the nominal one, we can compute the minimum temperature margin satisfied by the conductors. The results of the calculation are shown in Fig. 10 for a temperature margin of 1.94 K. Since the minimum quench energy depends on the temperature margin as  $\Delta T^{3/2}$ , the margin increase of 5% results in an enhance of 10% in terms of minimum quench energy.

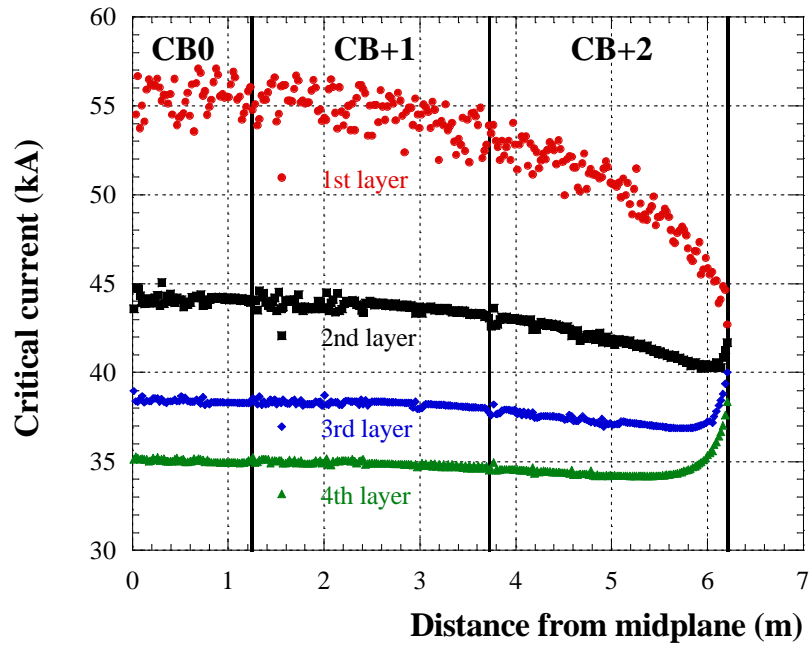


**FIG. 10:** Critical current as function of the distance from the magnet midplane and corresponding to the temperature margin  $\Delta T=1.94$  K.

## 6 CONCLUSIONS

The main result of the analysis is that the safety margins in temperature and critical current are well inside the requirements. Anyway, the suggestion again is to classify carefully the conductors in terms of their critical current, and to be sure to use the better lengths in the most critical region of the winding.

## REFERENCES

- (1) ANSYS<sup>®</sup>, Revision 5.5.2, Swanson Analysis Systems, Inc.
- (2) CMS Engineering Design Review, Saclay 2-4 December 1998, CMS 1998-148.